Reports of the Department of Geodetic Science

Report No. 233

METHODS FOR THE COMPUTATION OF DETAILED GEOIDS AND THEIR ACCURACY

by

Richard H. Rapp
and
Reiner Rummel

The Ohio State University
Department of Geodetic Science
1958 Neil Avenue
Columbus, Ohio 43210

November, 1975

Reports of the Department of Geodetic Science

Report No. 233

METHODS FOR THE COMPUTATION OF DETAILED GEOIDS AND THEIR ACCURACY

by

Richard H. Rapp

and

Reiner Rummel

The Ohio State University
Department of Geodetic Science
1958 Neil Avenue
Columbus, Ohio 43210

November, 1975

Foreword

This report was prepared by Professor Richard H. Rapp, and Reiner Rummel, Visiting Research Associate, Department of Geodetic Science, The Ohio State University. This work was supported through NASA, Contract No. NAS6-2484, The Ohio State University Research Foundation Project No. 3904 which is under the direction of Professor Richard H. Rapp. The contract supporting this research is administered through the Wallops Flight Center, Wallops Island, Virginia 23337.

Abstract

Two methods for the computation of geoid undulations using potential coefficients and $1^\circ \times 1^\circ$ terrestrial anomaly data are examined. It was found that both methods give the same final result but that the method suggested by Molodenskii allows a more simplified error analysis than the method used by Vincent and Marsh.

Specific equations were considered for the effect of the mass of the atmosphere and a cap dependent zero-order undulation term was derived. Although a correction to a gravity anomaly for the effect of the atmosphere is only about -0.87 mgal, this correction causes a fairly large undulation correction (e.g. 2.3 m with a cap size of 20°) that has not previously been considered.

The accuracy of a geoid undulation computed by these techniques was estimated considering anomaly data errors, potential coefficient errors, and truncation (only a finite set of potential coefficients being used) errors. It was found that an optimum cap size of 20° should be used.

The geoid and its accuracy were computed in the Geos-3 calibration area using the GEM6 potential coefficients and $1^\circ \times 1^\circ$ terrestrial anomaly data. The accuracy of the computed geoid is on the order of ± 2 m with respect to an unknown set of best earth parameter constants. This geoid was compared to that computed by Vincent and Marsh where we found a systematic difference of 3.9 m, an undulation difference variance of $(2.6\text{ m})^2$, and a maximum difference of 12 meters.

Preface

Under NASA contract NAS6-2484, we are to investigate the recovery of mean gravity anomalies from altimeter data that is obtained from Geos - 3. In developing the methods for such recovery it became clear that it could be helpful to have an external check on the altimeter determined geoid. This check could be obtained by computing geoid undulations from a combination of satellite and terrestrial gravity material. This latter set of geoid undulations could be used to remove systematic bias that might occur in the altimeter data due to orbit determination inaccuracies and errors in the altimeter itself.

Although work had been done in the computation of detailed geoids in the Geos - 3 calibration area (as well as other areas), no comprehensive analysis of the complete theoretical and numerical procedures has been carried out. Thus, as one of the first steps in our gravity anomaly recovery work we have prepared this report which attempts to define computational procedures for a detailed undulation computation and its accuracy in a precise way.

TABLE OF CONTENTS

	page
Foreword	ii
Abstract	iii
Preface	iv
1. Introduction	1
2. Details of Method A and B	1
2.1 Method A	1
2.2 Method B	5
3. The Effect of the Mass of the Atmosphere	6
4. Numerical Integration of Stokes' Equation	10
5. Accuracy Analysis	12
5.1 Introduction	12
5.2 Analysis for Method A	13
5.3 Analysis for Method B	15
6. Data Accuracy	16
6.1 Gravity Anomaly Accuracy	16
6.2 Potential Coefficient Accuracy	16
7. Optimum Cap Size	19
8. The Geoid in the Calibration Area	25
9. The Zero-Order Undulation	32
10. Summary	33
11. References	35

1. Introduction

The purpose of this report is to consider two procedures for the computation of detailed geoids using potential coefficients and 1°x1° terrestrial gravity material. In doing this we are interested in the results obtained from the two methods, as well as in the error analysis associated with each. The specific computation area is the Geos - 3 calibration area since for this area an accurate computation of the geoid undulation is needed. For our purposes the calibration area was considered to be between 40° and 20° north latitude and from 277° to 297° east longitude. Although the resulting geoid may not be the most accurate available geoid, in terms of data used for its computation, we intend the analysis given to demonstrate an accurate procedure for the computation of such a geoid.

Instead of giving extensive references to past work in this area we shall restrict ourselves to references directly applicable to the current discussion.

Method A for computing detailed geoid undulation has been used extensively by Vincent and Marsh (1974) and Marsh and Vincent (1973). A detailed accuracy analysis of Method A was given by Rapp (1973). Method B is described in Molodenskii, et.als. (1962, page 146) and Heiskanen and Moritz (1967, page 259) and has been used by Groten and Rummel (1974). Details of both methods will be given in subsequent sections.

2. Details of Method A and B

2.1 Method A

In Method A, the geoid is considered to be composed of three components N_1, N_2 and N_3 such that this sum yields the undulation:

$$N = N_1 + N_2 + N_3 \tag{1}$$

Specifically we have N_1 being the undulation implied by a given set of potential coefficients. The computation of such undulations has been discussed by Rapp (1971). There are two methods of interest here. The first, Method One, is based on the solution of the geodetic boundary value problem. The result is:

$$(2) \qquad N_1 = \frac{GM}{r\gamma} \sum_{\ell=2}^{\ell_{max}} \left(\frac{a}{r}\right)^{\ell} \sum_{m=0}^{\ell} (\bar{C}^{*}_{\ell m} \cos m\lambda + \bar{S}_{\ell m} \sin m\lambda)\, \bar{P}_{\ell m} (\sin\bar{\phi}).$$

where:

GM.....is the geocentric gravitational constant;
r.....is the geocentric distance to the point of which the undulation is being computed;
a.....is the equatorial radius;
γ.....is the normal gravity at the computation point;
$\bar{C}^{*}_{\ell m}$, $\bar{S}_{\ell m}$ are the differences between the actual potential coefficients and those implied by the adopted reference ellipsoid.

In Practice we have:

$$(3) \qquad \bar{C}^{*}_{2,0} = \bar{C}_{2,0(OBS)} - \bar{C}_{2,0(REF)}$$

$$(4) \qquad \bar{C}^{*}_{4,0} = \bar{C}_{4,0(OBS)} - \bar{C}_{4,0(REF)}$$

with all other C and S values equal to their observed values. In our computations the reference coefficients were computed from,

$$(5) \qquad \bar{C}_{2,0(REF)} = -J_2 / \sqrt{5}$$

$$(6) \qquad \bar{C}_{4,0(REF)} = -J_4 / \sqrt{9}$$

where the J coefficients are (Cook, 1959):

$$(7) \qquad J_2 = 2/3 \left(f(1 - f/2) - m/2(1 - 2f/7 + 11f^2/49)\right)$$

$$J_4 = -4/35 \; f(1 - f/2) \left(7f(1 - f/2) - 5m(1 - 2f/7)\right)$$

with:

$m = \omega^2 a^3 (1 - f)/ GM$

and:

ω is the angular velocity of the earth taken as $7.2921151467 \times 10^{-5}$ rad/sec.

We also note that in (2) P_{ℓ_n} is the fully normalized Legendre polynomial for the geocentric latitude $\overline{\varphi}$.

A second method for determining N_1 is to first find a r value that satisfies the following equation that describes the potential (W_0) of the geoid:

$$(8) \qquad W_0 = \frac{GM}{r}\left[1 + \sum_{\ell=2}^{\ell_{max}}\left(\frac{a}{r}\right)^{\ell}\sum_{m=0}^{\ell}\left(\overline{C}_{\ell_m}\cos m\lambda + \overline{S}_{\ell_m}\sin m\lambda\right)\overline{P}_{\ell_m}(\sin\overline{\varphi})\right] + \frac{\omega^2 r^2}{2}\cos^2\overline{\varphi}.$$

The solution for r is found by iteration in (8) after the geoid potential and other quantities in (8) are given. The undulation, N_1, is found by differencing r with the corresponding r of a specified reference ellipsoid. Specifically we have:

$$(9) \qquad N_1 = r - \frac{a\sqrt{1-e^2}}{\sqrt{1-e^2\cos^2\overline{\varphi}}}$$

The procedure using (8) and (9) is essentially that used by Vincent and Marsh. The results from this procedure will be the same as the results obtained from (2) provided that consistent constants of GM, a, ω, f, and W_0 are used. In both cases a zero-order undulation of the geoid is taken to be zero. (See section 9 where the removal of this restriction is discussed).

The N_2 component of (1) is computed in this method as follows:

$$(10) \qquad N_2 = \frac{R}{4\pi G}\iint_{\sigma_c}(\Delta\overline{g}^{\circ} - \Delta\overline{g}_s)\,S(\psi)\,d\sigma$$

where:

R.....is a mean earth radius (6371 km);
G.....is a mean value of gravity (979.8 gals);

$\overline{\Delta g^{p}}$ ..... is close to the mean free air anomaly and will be discussed in a subsequent section;

Δg_s ..... is the mean anomaly implied by the potential coefficients used in computing N_1 as in (2);

σ_c ..... is a limited cap about the computation point;

$S(\psi)$ ..... is the Stokes' function.

In practice the integration in (10) is replaced by a numerical integration. The value of Δg_s is:

$$(11) \qquad \overline{\Delta g_s} = \frac{1}{A} \iint_A \Delta g_s \delta A$$

where:

A ..... is the area in which the mean anomaly Δg_s is being determined. Specifically in the computation to be given here A will correspond to a $1^\circ \times 1^\circ$ mean anomaly. The value of Δg_s is computed from (Rapp, 1967):

$$(12) \qquad \Delta g_s = \frac{GM}{r^2} \sum_{\ell=2}^{\ell_{max}} (\ell-1) \left(\frac{a}{r}\right)^{\ell} \sum_{m=0}^{\ell} (\overline{C}^{*}_{\ell m} \cos m\lambda$$

$$+ \overline{S}_{\ell m} \sin m\lambda) \, \overline{P}_{\ell m} (\sin\overline{\phi}).$$

The actual evaluation of (11) with (12) was carried out by the analytic integration of the $\cos m\lambda$, $\sin m\lambda$ terms and the numerical integration of the $\overline{P}_{\ell m}$ term.

The N_3 term of (1) is formally given by:

$$(13) \qquad N_3 = \frac{R}{4\pi G} \iint_{\sigma-\sigma_c} (\overline{\Delta g^{p}} - \overline{\Delta g_s}) \, S(\psi) d\sigma.$$

where:

$\sigma-\sigma_c$ ..... represents the remaining global cap not included in σ_c. The cap σ_c is chosen in such a way that N_3 can be neglected. A cap size discussion will be given in section seven.

2.2 Method B

This method has been used by Groten and Rummel (1974), for detailed geoid computations. Here we write:

$$N = N_1' + N_2' + N_3' \tag{14}$$

where the primes have been used to distingiush these values from N_1, N_2, and N_3 given in (1). We have:

$$N_1' = \frac{R}{2G} \sum_{\ell=2}^{\ell_{max}} Q_\ell(\psi_o)\, \Delta g_\ell \tag{15}$$

where:

$Q_\ell(\psi_o)$.....is the Molodenskii truncation function (Heiskanen and Moritz, 1967, p.260) and is given as:

$$Q_\ell(\psi_o) = \int_{\psi_o}^{\pi} S(\cos\psi)\, P(\cos\psi) \sin\psi\, d\psi \tag{16}$$

where:

ψ_o.....is the cap size of gravity data to be included in N_2 and P_ℓ are the Legendre polynomials. In the computation to be given here we have use a program supplied by M. K. Paul based on his accurate and fast algorithm (Paul, 1973).

The value of Δg_ℓ is the ℓ'th degree component of the gravity anomaly implied by a set of potential coefficients and is given by:

$$\Delta g_\ell = \frac{GM}{r^2} (\ell-1) \left(\frac{a}{r}\right)^\ell \sum_{m=0}^{\ell} (\bar{C}^*_{\ell m} \cos m\lambda + \bar{S}_{\ell m} \sin m\lambda)\, \bar{P}_{\ell m}(\sin\vartheta). \tag{17}$$

We have for N_2':

$$N_2' = \frac{R}{4\pi G} \iint_{\sigma_c} \Delta\vec{g}\, S(\psi)\, d\sigma \tag{18}$$

where the σ_c cap has a radius ψ_0. The anomaly $\Delta\vec{g}$ is the same as in (10).

The N_3' term can be written as:

$$N_3' \quad \frac{R}{2G} \sum_{\ell=\ell_{max}+1}^{\infty} Q_\ell(\psi_0)\Delta g_\ell \tag{19}$$

This term represents the information above degree ℓ_{max} that has not been included in N_1'.

3. The Effect of the Mass of the Atmosphere

In developing the Stokes' equation for computing the disturbing potential or geoid undulation it was assumed that there were no masses external to the geoid. In fact, there are topographic masses and atmospheric masses. A consideration of the topographic masses can be made by alternate solution of the boundary value problem. It turns out that the corrections to the results of Stokes' equation are small except in mountainous areas. Specifically, the corrections are zero in ocean areas, such as being considered here. In any event, procedures for handling the topography in this type of computation are discussed in Moritz (1974, 1975) and are considered negligible for this paper.

In considering the atmosphere, we first define the potential of the geoid to be the sum of the gravity potential of the solid earth and oceans plus the potential of the atmosphere. Consequently, the computation of the geoid undulation using (8) requires that GM be that value including the mass of the atmosphere.

In the other phases of the geoid computations we must carry out the computations after the mass of the atmosphere has been removed from consideration, and then add any net effects back in. To solve this problem Moritz has shown that the mass of the atmosphere can be condensed onto the reference ellipsoid, so

that the mass of the latter will be equal to the mass of the solid earth and oceans plus the atmosphere. In this case equation (2), (12), and (17) are valid as they stand. To see this more clearly, we write the gravity potential at a point in the atmosphere as:

$$W = W^{\circ} + \frac{GM_A}{r} - G\int_r^{\infty} \frac{M(r')}{r'^2}\, dr' \tag{20}$$

where M_A is the mass of the atmosphere and $M(r')$ is the mass outside a sphere of radius r surrounding the earth. Equation (20) is written in slightly an approximated form. W° is the gravity potential due only to the solid earth plus oceans. The normal potential is now defined (approximately) as:

$$U = U^{\circ} + \frac{GM_A}{r} \tag{21}$$

where U° is the normal potential due to a reference ellipsoid that has a mass equal to that of the solid earth plus oceans. The disturbing potential, T, is:

$$T = W - U = W^{\circ} - U^{\circ} - G\int_r^{\infty} \frac{M(r')}{r'^2}\, dr' \tag{22}$$

$$T = T^{\circ} - G\int_r^{\infty} \frac{M(r')}{r'^2} dr' \tag{23}$$

where, in terms of potential coefficients:

$$T^{\circ} = \frac{GM}{r} \sum_{\ell=2}^{\ell_{max}} \left(\frac{a}{r}\right)^{\ell} \sum_{m=0}^{\ell} (\bar{C}^{*}_{\ell m} \cos m\lambda + \bar{S}_{\ell m} \sin m\lambda)\, \bar{P}_{\ell m}(\sin\bar{\phi}). \tag{24}$$

The second term on the right hand side of (23) can be evaluated numerically. For

the case of r referring to the surface of the ellipsoid, the second term has a value of about 0.006 kgal meter which would be about 0.6 cm in geoid height. Thus this term is negligible. Consequently, we can use (24) dividing by γ to obtain N (from potential coefficients). The resultant expression is (2).

The computation of the gravity anomaly in the case that the atmosphere is condensed onto the ellipsoid can be expressed as:

$$\Delta g = \Delta g^{\circ} + \delta g_A \tag{25}$$

where:

Δg°.....would be the gravity anomaly in a system where all atmosphere mass is condensed into the ellipsoid;

Δg.....would be the usual anomaly where the atmosphere is not condensed into the ellipsoid.

δg_A.....is a correction that can be computed knowing the elevation of the point and a model for the atmosphere.

In terms of potential coefficients, Δg° is given by (12), or by degree in terms of (17). Consequently, the computation of $\Delta \bar{g}_s$ in (10) or Δg_ℓ in (15) is not affected by the condensation of the atmosphere mass to the ellipsoid.

The anomaly to be used in the Stokes' integration based on terrestial data, must be one to which the atmosphere correction term has been applied. Specifically, we must use in (10) and (15):

$$\Delta \bar{g}^{\circ} = \Delta \bar{g} - \delta \bar{g}_A \tag{26}$$

where:

$\Delta \bar{g}$.....will be the usually given free-air anomaly and;

$\delta \bar{g}_A$.....will be given based on the mean height of the (in our case) $1^{\circ} \times 1^{\circ}$ block.

Values of δg_A can be taken as $-\delta g$ where δg is tabulated for the Geodetic Reference System 1967 (IAG, 1971). If we assume that δg_A is constant within the integration cap used in the Stokes' integration, the effect of the atmosphere on the geoid undulation is:

$$\delta N_A = \frac{-R\delta g_A}{4\pi G} \iint_{\sigma_0} S(\psi)\, d\sigma \tag{27}$$

Since (27) is evaluated in a circular cap whose radius is ψ_0, we can write (27) in the form:

$$\delta N_A = \frac{-R\delta g_A}{2G} \int_0^{\psi_0} S(\psi) \sin\psi\, d\psi \tag{28}$$

Equation (28) can be written in the form:

$$\delta N_A = -\frac{R}{G}\delta g_A \cdot \mathfrak{F}(\psi_0) \tag{29}$$

where:

$$\mathfrak{F}(\psi) = \tfrac{1}{2}\int_0^{\psi} S(\psi) \sin\psi\, d\psi \tag{30}$$

which is evaluated and tabulated in Lambert and Darling (1936). Using these values of $\mathfrak{F}(\psi_0)$ and values of δg_A from the Geodetic Reference System 1967; the following δN_A values were computed.

Table One. Effect of Atmosphere on Geoid Undulation Computations (meters)

	Mean Elevation of Cap (meters)				
ψ_0	0	100	200	300	400
5°	0.56	0.56	0.55	0.55	0.54
10°	1.17	1.16	1.14	1.13	1.12
15°	1.75	1.73	1.71	1.69	1.67
20°	2.26	2.23	2.21	2.18	2.16
25°	2.67	2.64	2.61	2.58	2.55
30°	2.97	2.93	2.90	2.87	2.83

The corrections in Table One should be added to the undulation component computed from (10) and (18) when $\Delta\bar{g}^{\circ}$ is taken simply as the observed free air anomally, $\overline{\Delta g}$.

From Table One we see that the correction is quite sensitve to the cap size, but insensitive to the elevation within the range tested.

In the actual geoid computations to be made for this report, 70% of the gravity material is in ocean areas where the elevation would be zero. The remaining areas would be in the eastern and central United States, which have a small mean elevation. Consequently, for this report we will use the δN_A value for a mean elevation of 0 meters. A more accurate procedure would require knowledge of the 1° x 1° mean elevations. For this report this is not necessary, but for high elevation continental areas, such accurate computation for various cap sizes needs to be done in the future.

4. Numerical Integration of Stokes' Equation

The evaluation of (10) or (18) is carried out by summation in which an average $S(\psi)$ value is needed. We write (18) (for example) as:

$$N_2 = \frac{R}{4\pi G} \sum \Delta\bar{g}^{\circ}\, \overline{S(\psi)}\, \Delta\sigma \tag{31}$$

where:

$\Delta\sigma$..... is the area of the 1° x 1° block and:

$$S(\psi) = \frac{1}{\Delta\sigma} \iint_{\Delta\sigma} S(\psi)\delta\sigma \tag{32}$$

In practice (32) is evaluated by computing one, or several values of $S(\psi)$ from the computation point to points in the block in which $\Delta\bar{g}^{\circ}$ is given, and meaning the result. The number of values meaned will depend on the size of ψ and the accuracy desired. Since $S(\psi)$ changes rapidly for small ψ values, more points are required for an accurate mean when ψ is small than when ψ is large.

To investigate a proper integration procedure, we equate the undulation (in equation form) obtained by Method A and Method B. The following equality should then hold:

$$(33) \qquad \frac{R}{4\pi G} \iint_{\sigma_c} \Delta\bar{g}_c^{\circ} S(\psi)\, d\sigma = \frac{GM}{2Gr} \sum_{\ell} \left(\frac{a}{r}\right)^{\ell} (1-Q_{\ell}) \sum_{m} (\bar{C}^{*}_{\ell m} \cos m\lambda + \bar{S}_{\ell m} \sin m\lambda)\, \bar{P}_{\ell m}(\sin\bar{\phi}).$$

Using the GEM 6 potential coefficients to $\ell = 16$, the right hand side of (33) can rigorously be computed yielding a "true" value. The left hand side of (33) can be evaluated by subdivision schemes until one is found that yields results consistent with the "true" value. Four subdivision schemes were tested:

Subdivision One (1): Stokes' function is computed only for the center point of each anomaly block (the undulation computation point is at the corner of a $1^{\circ} \times 1^{\circ}$ block);

Subdivision Two (4-1): Inside a spherical cap of $\psi = 2^{\circ}$ around the computation point every $1^{\circ} \times 1^{\circ}$ block is divided into four equal (in terms of latitude/longitude increments) blocks for which the Stokes' function is evaluated at the center point and meaned. Outside $\psi = 2^{\circ}$, the Stokes' function is evaluated based only on the center point of the $1^{\circ} \times 1^{\circ}$ block.

Subdivision Three (16-4): Inside a spherical cap of $\psi = 2^{\circ}$ a 16 sub-block system is used, while beyond 2° a 4 sub-block system is implemented.

Subdivision Four (64-16-4-1): The following sub-block system is used here:

$\psi \leq 2^{\circ}$; 64 sub-blocks
$2^{\circ} < \psi \leq 5^{\circ}$; 16 sub-blocks
$5^{\circ} < \psi \leq 10^{\circ}$; 4 sub-blocks
$10^{\circ} < \psi < 20^{\circ}$; 1 sub-block

Using these various sub-division schemes, the left hand side of (33) was evaluated

with the results shown in Table Two, along with the "true" value computed from the right hand side of (33), for four points in the calibration test area.

Table Two. Influence on Undulation Computation of Various Subdivision Schemes Used in the Evaluation of the Stokes' Formula. (meters)

	Test Point (φ, λ)			
Subdiv.Model	1(40°, 277°)	2(40°, 297°)	3(20°, 277°)	4(20°, 297°)
1	-18.4	-26.8	4.0	-52.1
2	-18.4	-26.9	4.1	-52.5
3	-18.4	-27.0	4.1	-52.8
4	-18.5	-27.0	4.2	-52.9
"true"	-18.5	-27.1	4.2	-53.0

The best agreement with the "true" value exists for subdivision model four, which is thus chosen for use in the actual geoid computations in the calibration area. Since the actual integration error will depend on the magnitude of the anomalies in the Stokes' kernal, we would expect Method A would be somewhat less sensitive to integration errors than Method B, since in A an anomaly difference is used while in Method B, the actual anomaly is used. The exact sensitivity will depend on the magnitude and smoothness of Δg_s used in A (or in other words on the value of ℓ_{max}). Consequently, we recommend the above subdivision model for use in either Method A or Method B of undulation computation.

5. Accuracy Analysis

5.1 Introduction

In this section we will try to estimate the accuracy of the geoids computed by the methods described in section two. In such an analysis we will try to estimate the optimum truncation angle ψ_0. Several of the error terms have been discussed previously (Rapp, 1973) but they will be rediscussed here for the specific area of computation.

There are basically two data source errors. These arise from the errors in the potential coefficients, and the errors in the gravity anomalies. The vari-

ance-covariance matrix of the potential coefficients is designated Σ_c, and that of the anomalies as $\Sigma\Delta g$. We will assume that these matrices are diagonal. This assumption is true for the gravity anomalies since they are estimated independently, but not exactly true for the potential coefficients.

5.2 Analysis for Method A

Method A is represented by (1). The first two terms on the right hand side of (1) represent errors of commission, while N_3 represents an error of ommission. For a single undulation error variance we write:

$$\sigma^2 = \sigma_c^2 + \sigma_o^2 \tag{34}$$

where:

σ_c .....is associated with the commission errors;
σ_o .....is associated with the ommission errors.

There should be no confusion with this σ_c and that used previously to designate the integration cap. To compute σ_c we write:

$$N_c = N_1 + N_2 \tag{35}$$

Considering (2) and (10), (35) can be written in matrix form as:

$$N_c = \underline{B}^T \underline{C} + \underline{A}^T (\underline{\Delta g}^o - \underline{\Delta g}_c) \tag{36}$$

where the elements of B are the coefficients of the potential coefficients (designated C in (36)). The elements of A are taken from (10). We can represent the computation of Δg_3 as:

$$\underline{\Delta g}_3 = \underline{B}_3^T \underline{C} \tag{37}$$

where the elements of $\underline{B}_3$ are found as the coefficients of the potential coefficients in (12). Inserting (37) into (36) we have:

$$N_3 = \underline{B}^T \underline{C} + \underline{A}^T \underline{\Delta g}^0 - \underline{A}^T \underline{B}_1^T \underline{C} \tag{38}$$

Applying the propagation of error formulas we have:

$$\sigma_0^2 = \underline{B}^T \underline{\Sigma}_{\Delta g} \underline{B} + \underline{A}^T \underline{\Sigma}_{\Delta g} \underline{A} + \underline{A}^T \underline{B}_1^T \underline{\Sigma}_{\Delta g} \underline{B}_1 \underline{A} \tag{39}$$

$$- 2 \underline{B}^T \underline{\Sigma}_{\Delta g} \underline{B}_1 \underline{A}.$$

The evaluation of this equation is complex and will not be attempted in this report, as a simpler formula will be found when using Method B for the undulation computation.

The specific evaluation of N_3 can not be done as we do not know the high degree potential coefficients. At best we can find a global average effect by writing (Rapp, 1973):

$$\sigma_0^2 = \frac{R^2}{4G^2} \sum_{\ell=\ell_{max}+1}^{\infty} s^{(\ell+2)} Q_\ell^2(\psi) c_\ell(\Delta g) \tag{40}$$

where $c_\ell(\Delta g)$ are anomaly degree variances and s is (Tscherning and Rapp, 1974): 0.999617. Although the summation is taken to ∞, in practice we would take the summation to about 200 as we are using 1° data as the smallest terrestrial data block. For $\psi = 10°$, we get for σ_0^2 about 1.1 meters and for $\psi = 20°$, about 0.7 meters.

Other error sources in the computation of point undulation include (for the computation in this paper) the fact that smaller anomalies than 1° x 1° anomalies may be needed, and that the reference set of constants may yield an equatorial gravity different from that implied by the best set of constants. These effects have been discussed in Rapp (1973). For our purposes we will assume that 1° x 1° data is the only data used: (there appears to be about ±0.4 m of more detailed information in ano-

maly data in blocks smaller than 1° x 1°); and we will assume our equatorial gravity is true; if it is not, errors up to 2.6m($\psi = 20°$) for a 1 mgal error in equatorial gravity can be expected, exclusive of N_o considerations (see sec. 9).

5.3 Analysis for Method B

As in Method A, we have for Method B errors of commission and errors of ommission. The commission errors arise in (15) and (17) due to potential coefficient errors, and in (18) due to anomaly errors. The ommission error is caused by the fact that the summation in (15) is taken to ℓ_{max} instead of ∞. Th s latter error is the same as given in (40) and the discussion given with respect to (40) is equally valid here.

To carry out this analysis we express the computational procedure in the form:

$$N_o = \underline{B}' \underline{Q} \underline{C} + \underline{A}' \underline{\Delta g}^o \tag{41}$$

where:

.....A, B, and C are as before and Q is a diagonal matrix whose elements are composed of values of $Q_\ell(\psi_o)$. Error propagation thru (41) yields for Method B:

$$\sigma_o^2 = \underline{B}' \underline{Q} \, \Sigma_{\underline{c}_s} \, \underline{Q}' \underline{B} + \underline{A}' \Sigma \Delta g \, \underline{A} \tag{42}$$

Comparing (42) with the corresponding result (39), for method A indicates that the error analysis for method B is considerably simpler than for method A. The actual implementation of (42) can be done through minor modifications of programs used in the evaluation of (15) and (18) since Σ_{c_s} and $\Sigma \Delta g$ are to be regarded as diagonal matrices. The accuracy of the geoid we will compute will be evaluated using (42) and (40) in (34).

6. Data Accuracy

6.1 Gravity Anomaly Accuracy

The gravity data to be used in these computations will be 1° x 1° mean anomalies. Each of these anomalies that has been estimated has an assigned standard deviation. In some cases an anomaly will be needed, within a cap, for which no estimate of that anomaly is available. In this case we will assume that the anomaly is zero and that its standard deviation is ± 30 mgals, which is the root mean square variation of 1° x 1° mean free-air gravity anomalies.

The 1° x 1° data distribution within and around the calibration area is shown in Figure One. In this Figure One, zero (0) indicates those blocks for which an anomaly estimate is available and an * indicates that no anomaly exists. The outer borders of a 10° cap and a 20° cap are also shown.

6.2 Potential Coefficient Accuracy

The formal standard deviations for the GEM 6 potential coefficients were provided to us by Frank Lerch. These formal statistics are considered optimistic and we therefore used two approaches in estimating realistic standard deviations for the potential coefficients.

In the first approach the formal standard deviations were multiplied by a scale factor of 3.4 as suggested by Lerch, et. als. (1974). An average percentage error, by degree, can be defined as:

$$(\overline{\%})_\ell = \frac{\mathrm{RMS}\,(m_{c,s})_\ell}{\mathrm{RMS}\,(\overline{C,S})_\ell} \tag{43}$$

where:

RMS $(m_{c,s})$ ... is the root mean square value of the standard deviation of the coefficients of degree ℓ, and,

RMS (C,S) ... is the root mean square value of the cofficients of the GEM 6 solution of degree ℓ.

Values of (43) are plotted in Figure Two where it is seen that the percentage error increases so that it is about 80% at ℓ = 16, and even higher for the coefficients above 16 to 22.

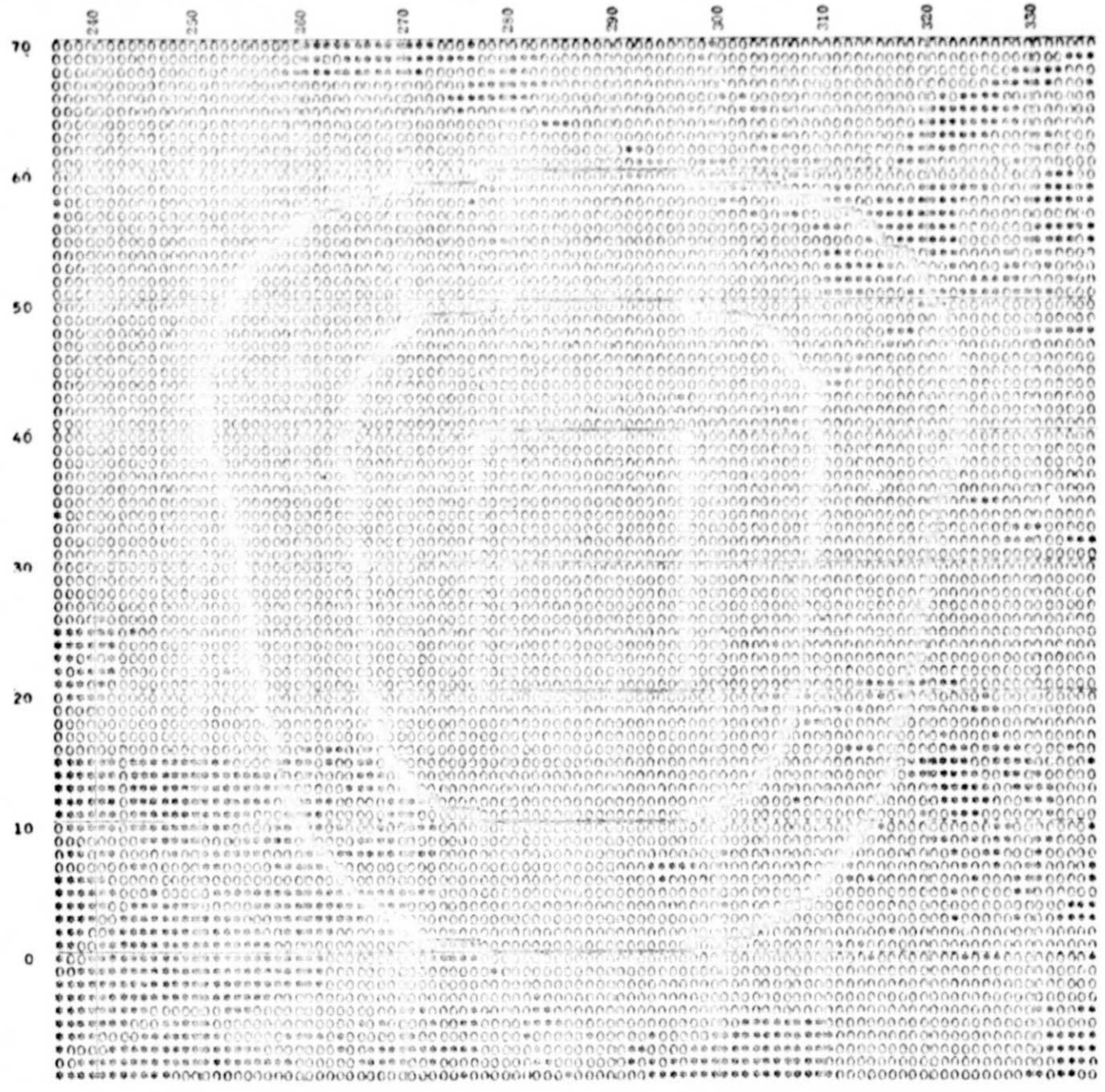

Figure One. $1^\circ \times 1^\circ$ data distribution within and around the calibration area. Outer borders of calibration area, 10° cap and 20° cap are shown.
•.....block where no anomaly was available
0.....block with an anomaly estimate

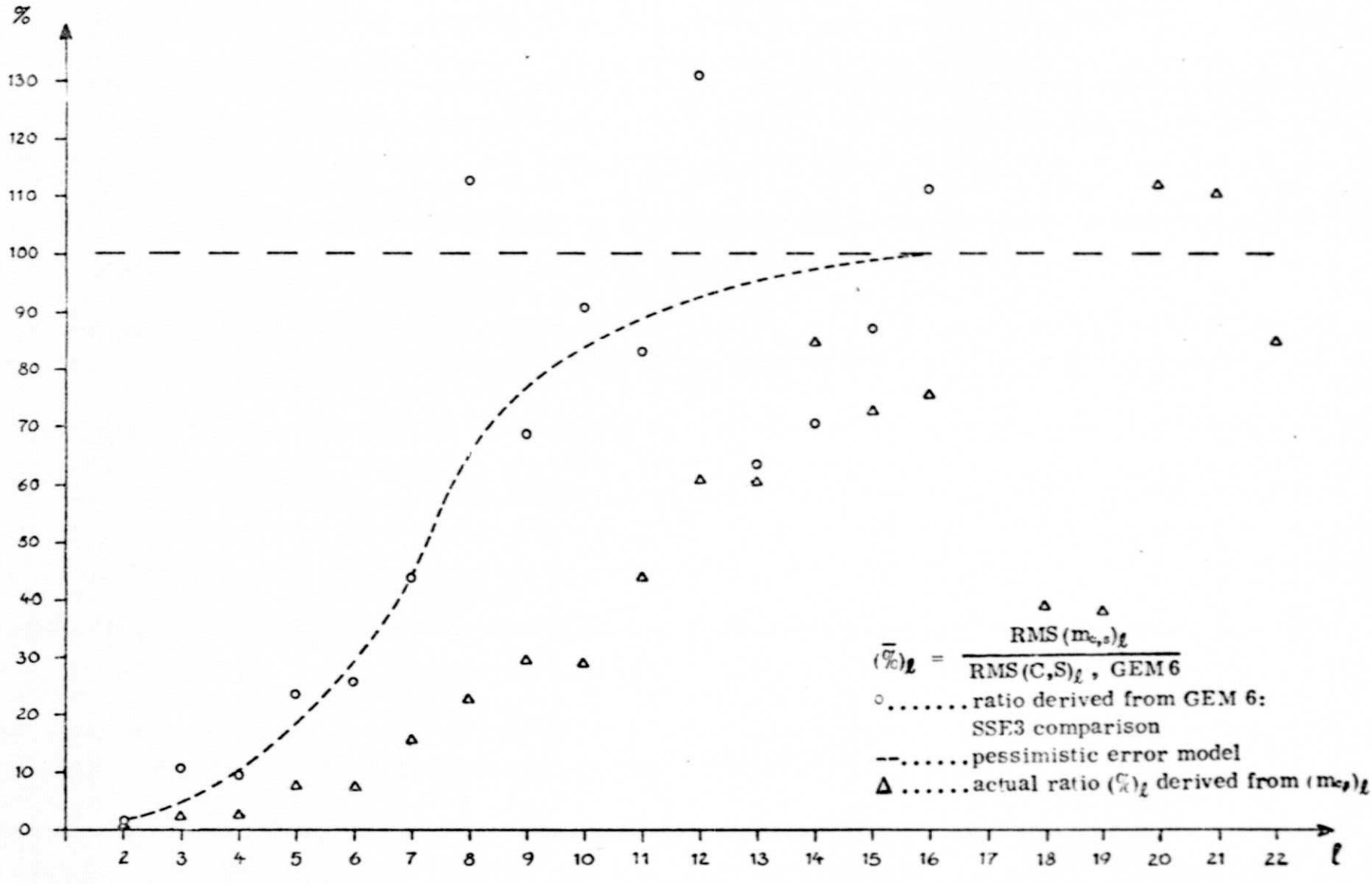
%
130
120
110
100
90
80
70
60
50
40
30
20
10
0
2
3
4
5
6
7
8
9
10
11
12
13
14
15
16
17
18
19
20
21
22
ℓ
$(\bar{\%})_\ell = \frac{RMS(m_{c,s})_\ell}{RMS(C,S)_\ell\ ,\ GEM\ 6}$
°.....ratio derived from GEM 6: SSE3 comparison
--.....pessimistic error model
Δ .....actual ratio $(\%)_\ell$ derived from $(m_{c,s})_\ell$

Figure Two.

A second approach to potential coefficient accuracy determination starts with determining the percentage difference, by degree, between the GEM 6 coefficients and the coefficients of the Standard Earth III (Gaposchkin, 1974). This difference increases to a maximum of 130% at degree 12 as seen in Figure Two. With these differences a curve was drawn to represent the percentage accuracies with the specification that this percentage be 100% at degree 16. We then could estimate the standard deviation of the potential coefficients (but only by degree) by multiplying the root mean square coefficient value by the percentage error. Clearly, this second approach yields accuracy estimates more pessimistic than found in the first approach.

7. Optimum Cap Size

We now wish to determine an optimum ψ_0 that gives a minimum error in the determination of the geoid undulation. In order to do this we consider the various error sources that are associated with method B.

First we consider the commission error due to the errors in the gravity anomalies. This error will clearly depend on the geographic location of the computation point. In order to obtain a representative value, computations were carried out for nine representative points in the calibration area, as the cap size was varied from 0° to 30°. The standard deviations for the nine points were averaged and are plotted as a function of ψ in Figure Three. We see that the standard deviation, due to the anomalies increases from ±0 meters at $\psi = 0°$ to 1.2 meters at $\psi = 30°$.

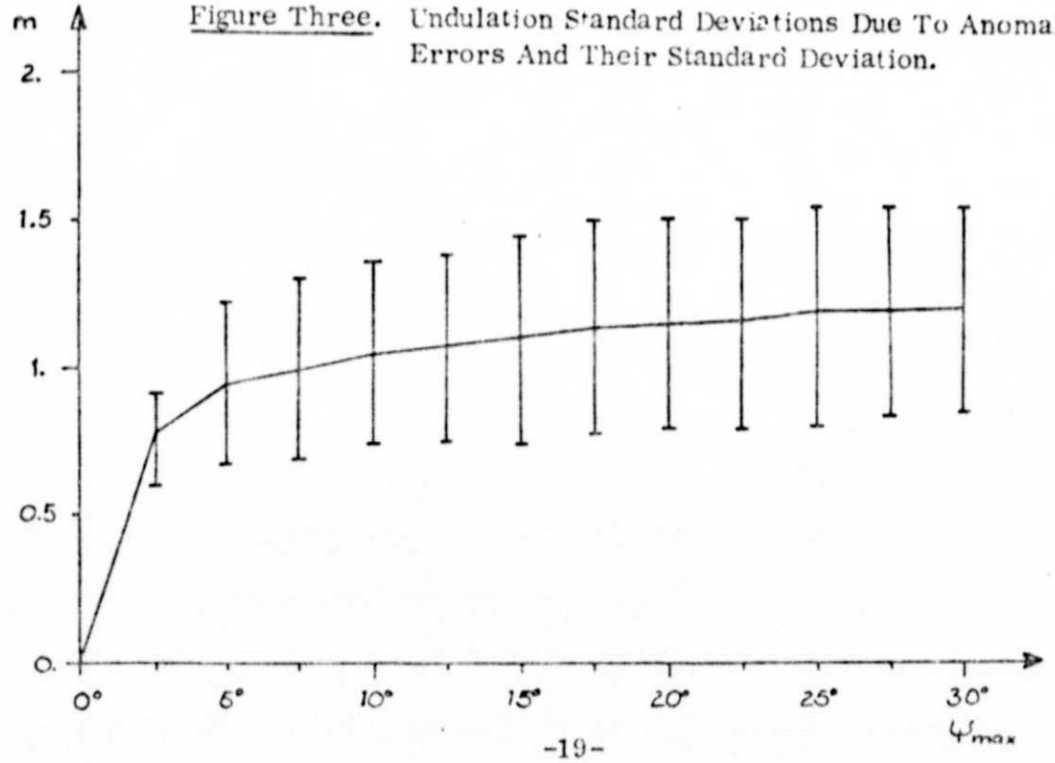

Figure Three. Undulation Standard Deviations Due To Anomaly Errors And Their Standard Deviation.

We next consider the commission errors due to the potential coefficien's. Again values have been computed at nine points and averaged to obtain a representative number. Specifically, we have made computations for different ℓ_{max} values and different ψ values for the two error models of the GEM 6 solution previously discussed in section 6.2. The resulting standard deviations are shown in Figure Four for error model one with $\ell_{max} = 8$, 12, 16 and 22, and for $\ell_{max} = 16$ with error model two. Values are also given in Table Three.

In computing the values for the $\ell_{max} = 22$ solution it is necessary to adopt standard deviations for the potential coefficients not present in the GEM 6 set as we have in essence assumed these coefficients to be zero. Specifically, we have taken for their standard deviation, the root mean square coefficient variation implied by the following anomaly degree variance model given in Tscherning and Rapp (1974, p. 20):

$$c_\ell = \frac{A(\ell-1)}{(\ell-2)(\ell+B)} \tag{44}$$

with $A = 425.28$ mgal^2, and $B = 24$.

Table Three. Undulation Standard Deviations Due to Potential Coefficient Errors. (meters)

	$\ell_{max} = 8$		$\ell_{max} = 12$		$\ell_{max} = 16$		$\ell_{max} = 22$
	Error Model		Error Model		Error Model		Error Model
ψ°	1	2	1	2	1	2	1
0	1.3	3.7	2.0	5.0	2.8	5.7	3.7
2.5	1.0	2.8	1.3	3.4	1.5	3.6	1.6
5.0	0.7	1.9	0.7	2.0	0.8	2.0	1.3
7.5	0.5	1.2	0.6	1.4	1.1	1.8	1.7
10.0	0.4	0.9	0.7	1.6	1.2	2.1	1.4
12.5	0.4	1.0	0.8	1.6	1.1	2.1	1.2
15.0	0.4	1.2	0.8	1.9	0.8	2.0	1.1
17.5	0.4	1.3	0.6	1.7	0.7	1.7	1.0
20.0	0.4	1.2	0.5	1.4	0.7	1.5	0.8
22.5	0.4	1.1	0.4	1.2	0.6	1.3	0.7
25.0	0.3	0.9	0.4	1.0	0.5	1.1	0.6
27.5	0.3	0.8	0.3	0.9	0.4	0.9	0.5
30.0	0.2	0.6	0.3	0.7	0.3	0.8	0.4

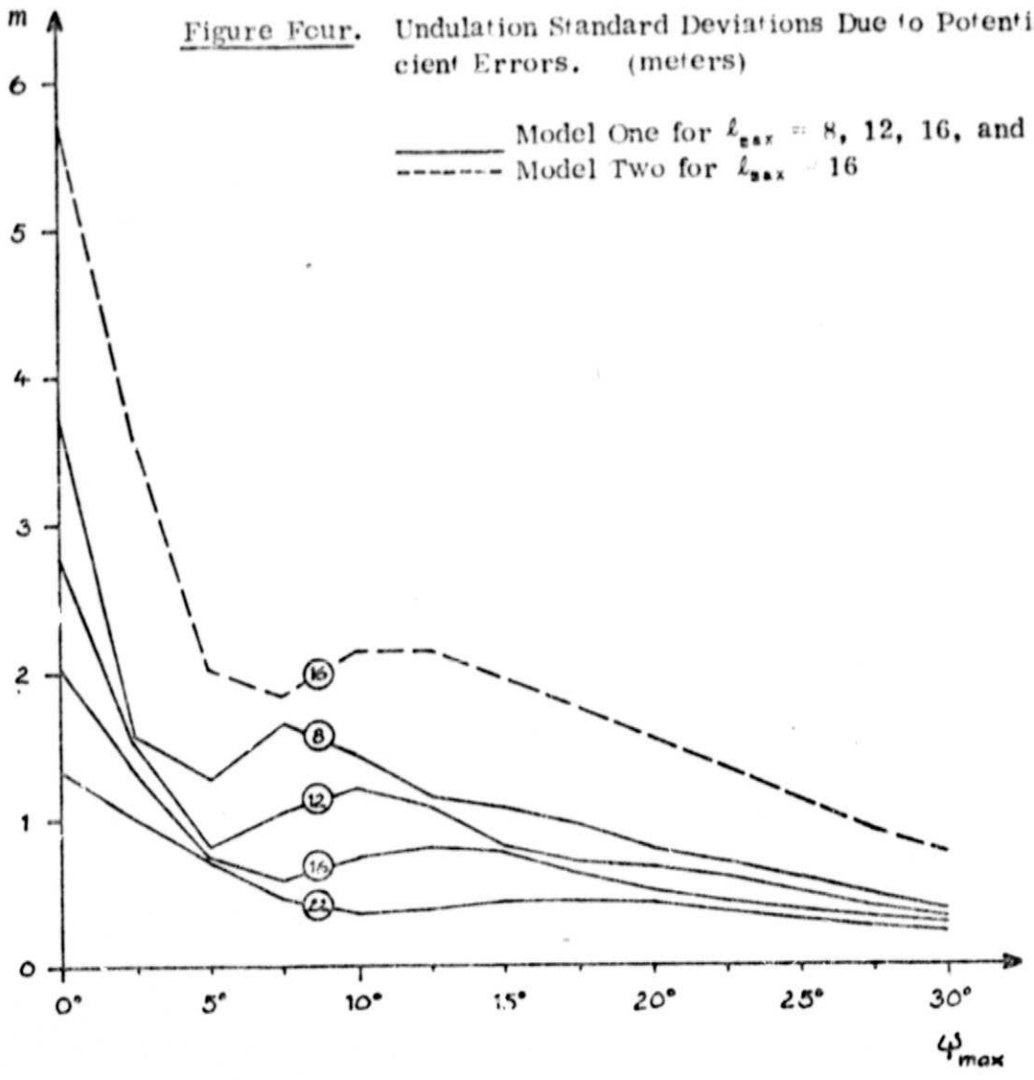

Figure Four. Undulation Standard Deviations Due to Potential Coefficient Errors. (meters)

_____ Model One for ℓ_{max} = 8, 12, 16, and 22
------- Model Two for ℓ_{max} = 16

The differences in the results from the two error models have a maximum at $\psi = 0°$ and decreases as ψ increases.

The last error source considered here is that due to the neglect of the higher degree potential coefficients. This error is given by (40) where the summation is taken to 200 and (44) was used for the anomaly degree variance model. These results are given in Table Four and Figure Five for various ℓ_{max} and ψ values.

Table Four. Undulation Error Caused by Potential Coefficient Truncation at Specified ℓ_{max}. (meters)

	ℓ_{max}			
$\psi°$	8	12	16	22
0	7.6	5.5	4.4	3.3
2.5	3.5	1.8	1.2	1.0
5.0	2.1	1.9	1.8	1.4
7.5	2.6	2.3	1.7	0.9
10.0	2.9	2.1	1.2	0.8
12.5	2.9	1.6	1.0	0.8
15.0	2.5	1.1	1.0	0.6
17.5	2.0	1.1	0.9	0.5
20.0	1.5	1.0	0.7	0.5
22.5	1.2	1.0	0.5	0.4
25.0	1.0	0.8	0.5	0.3
27.5	0.8	0.5	0.4	0.3
30.0	0.7	0.4	0.3	0.2

We can now quadratically add the three error sources together to obtain the final representative undulation standard deviation in the calibration area. The resultant standard deviations are plotted in Figure Six.

In considering Figure Six for the 8, 12, 16, and 22 solutions with potential coefficient error model one we see that the error at first decreases as ψ increases, then it increases somewhat and finally decreases. At certain ψ values such as 7.5° for ℓ_{max} 12 we would expect a larger error than at smaller or larger ψ values. This would indicate that one should choose an optimum ψ value based on the ℓ_{max} of the potential coefficient field being used. Based on Figure Six we feel a ψ 20° cap is reasonable.

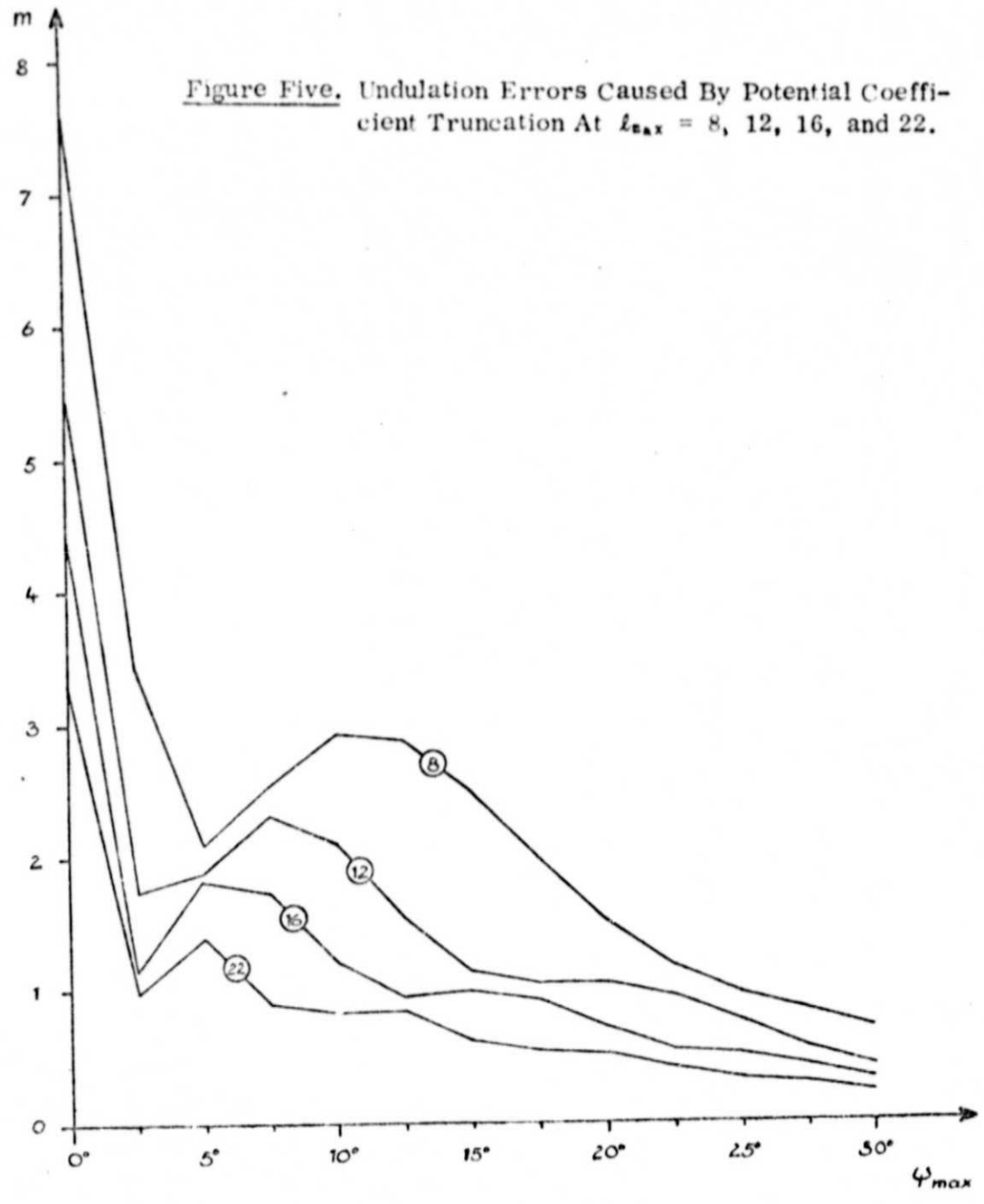

Figure Five. Undulation Errors Caused By Potential Coefficient Truncation At ℓ_{max} = 8, 12, 16, and 22.

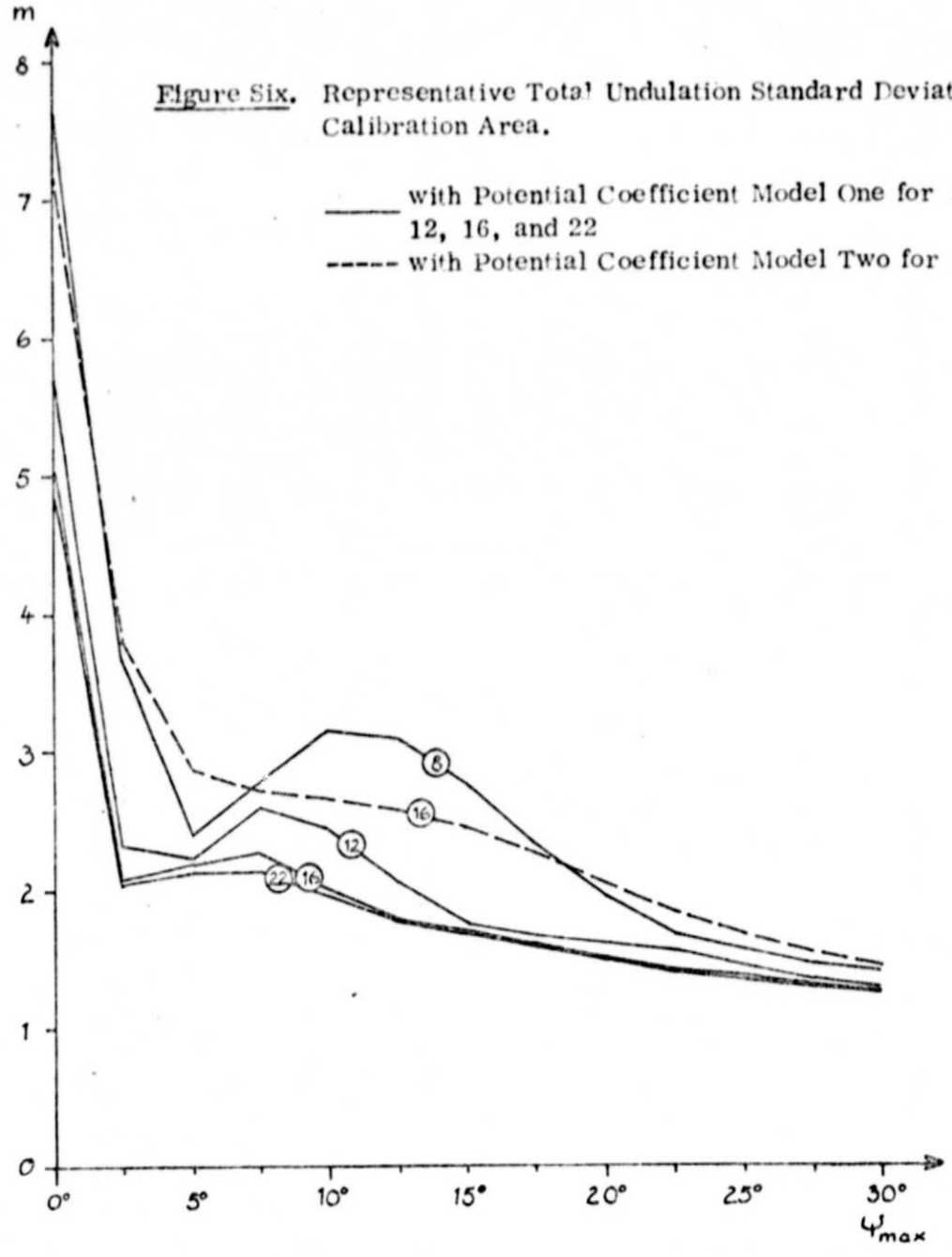

Figure Six. Representative Total Undulation Standard Deviation in the Calibration Area.

_____ with Potential Coefficient Model One for ℓ_{max} = 8, 12, 16, and 22

----- with Potential Coefficient Model Two for ℓ_{max} = 16

The standard deviation of the undulation when the pessimistic error model for the potential coefficients is used is shown in Figure Six for the case of ℓ_{max} = 16. Although the errors are larger, the difference decreases as ψ increases so that at ψ = 20° and ℓ_{max} 16, the total standard deviation of the undulation using the optimistic potential coefficient error model is ±1.5 m while it is ±2.1 m when using the pessimistic error model.

For the final undulation computations the GEM 6 solution was used with $\ell_{max} = 16$. This was done so that the error analysis could be done without making assumptions about the coefficients between degree 17 and 22 not estimated in the GEM 6 solution. It will be shown that no significant undulation difference occurs when using a $\ell_{max} = 16$ or 22 in the case of the GEM 6 set.

8. The Geoid in the Calibration Area

The previous discussions have dealt with the method for detailed undulation computation and the method of accuracy analysis. We now turn to the computation of the detailed geoid and its accuracy in the calibration area using the GEM 6 potential coefficients and $1° \times 1°$ gravity anomalies given to a mgal on a tape dated July 1975.

We first define a set of constants identical to that used by Marsh and Vincent (1973) so that our undulations may be compared. These constants are:

$$\begin{aligned} \omega &= 7.2921151467 \times 10^{-5} \text{ rad/s} \\ a &= 6378142 \text{m} \\ f &= 1/298.255 \\ GM &= 3.986009 \times 10^{14} \text{ m}^3/\text{s}^2 \\ W_0 &= 6263687.52 \text{ kgal m} \\ \gamma_e &= 978032.14 \text{ mgal} \end{aligned}$$

The GM includes the mass of the atmosphere* and thus the effect of the atmosphere is included in the geoid potential W_0 and equatorial gravity, γ_e. The normal gravity formula corresponding to these constants is then:

$$\gamma_{new} = \gamma_e (1 + 0.0053024269 \sin^2\varphi - 0.0000059 \sin^2 2\varphi) \tag{45}$$

Now the anomalies on the July 1975, 1° tape were given with respect to the gravity formula of the Geodetic Reference System 1967 and thus need to be converted to be given with respect to the new constants. We have:

* If it did not, then the $\overline{N}_0$ term from equation (51) would have to be evaluated.

(46) $$\Delta g_{new} = \Delta g_{67} + \gamma_{67} - \gamma_{new}$$

or numerically:

(47) $$\Delta g_{new} = \Delta g_{67} - 0.29 - 0.06 \sin^2\phi \text{ mgal}$$

Although this correction is small, it is systematic and its neglect could cause errors on the order of 0.8 meters in the computed undulation.

For the final results several different computations were performed using the GEM 6 potential coefficients and the 1°x 1° mean anomalies converted to a gravity formula consistent with the adopted constants. We first computed the geoid undulations using Method B with the GEM 6 coefficients truncated at degree 16 and with a cap size of 20°. These undulations are given in Table Five and in contour form in Figure Seven. These undulations include an atmospheric correction of 2.26 m obtained from Table One. The undulation standard deviations for the calibration area when using the potential coefficient error model one is shown in Table Six and when using the potential coefficient error model two in Table Seven. In the first case the standard deviations have a maximum of ±2.0 m with a minimum standard deviation of ±1.1 m. The corresponding values when using the second error model are ±2.4 m and ±1.8 m. These error estimates are all given with respect to the adopted set of constants, and exclude the error contribution due to the neglect of detailed gravity information in blocks below 1° x 1° in size. The accuracy of these standard deviations depends on how well the accuracy models for the anomalies, potential coefficients and truncation effects have been handled. We believe that the latter two effects have been handled reasonably. However, the anomaly error contribution has been based on the anomaly standard deviations that may be optimistic.

We next computed the geoid undulations using Method A described in section 2.1 with the identical data as used in Method B. A comparison of the resultant geoids showed a maximum descrepency of 0.2 m with other statistics on the comparison given in Table Eight. We conclude that either method consistently applied will give the same undulation at the ±0.1 meter level.

A computation was made using method B when a truncation angle of 10° was used instead of 20°. The largest difference found was 3.6 meters with the

	λ = 280							285							290							295				
φ = 40	-33.7	-33.8	-33.6	-32.6	-32.2	-32.6	-32.7	-32.5	-32.0	-31.4	-31.6	-32.3	-32.9	-32.2	-31.8	-31.1	-30.1	-30.1	-30.6	-30.6	-29.6					
	-33.4	-33.7	-33.1	-31.9	-32.4	-32.7	-32.4	-32.9	-33.1	-33.5	-34.9	-36.1	-36.2	-36.0	-35.7	-35.7	-34.9	-33.9	-33.3	-32.1	-30.5					
	-33.0	-32.8	-32.2	-31.7	-31.8	-31.9	-32.7	-34.4	-34.9	-35.8	-36.1	-39.1	-38.7	-38.3	-38.1	-37.8	-36.7	-35.3	-34.0	-32.3	-30.9					
	-32.0	-31.9	-32.1	-32.3	-31.7	-32.3	-34.2	-36.1	-36.7	-38.0	-40.0	-40.5	-40.8	-40.6	-40.3	-39.7	-38.2	-36.4	-34.7	-33.3	-32.3					
	-30.8	-31.5	-32.2	-32.0	-32.3	-34.1	-35.9	-37.3	-38.7	-40.6	-41.9	-42.4	-42.0	-41.5	-41.2	-40.3	-38.9	-37.1	-35.4	-34.2	-33.2					
35	-30.0	-31.0	-31.4	-31.8	-33.6	-35.7	-37.0	-38.4	-40.9	-43.3	-44.1	-43.9	-43.4	-42.7	-42.2	-41.3	-39.7	-37.7	-35.8	-34.5	-33.6					
	-29.5	-30.6	-31.9	-33.0	-35.0	-37.1	-38.1	-40.2	-43.6	-45.5	-46.2	-46.1	-45.4	-44.5	-43.3	-42.2	-40.7	-38.6	-36.3	-34.8	-33.9					
	-29.2	-30.2	-31.7	-33.3	-35.3	-37.2	-38.0	-41.7	-45.2	-47.4	-48.4	-48.4	-47.6	-46.4	-45.1	-43.5	-41.9	-39.6	-36.0	-34.2	-33.9					
	-29.6	-29.4	-31.2	-33.0	-35.3	-37.2	-39.2	-41.9	-44.4	-47.9	-49.4	-49.6	-49.0	-48.0	-46.6	-45.3	-43.8	-41.2	-37.7	-36.1	-35.7					
	-29.9	-29.0	-30.5	-32.7	-35.5	-37.6	-40.3	-42.6	-43.8	-46.6	-49.1	-49.7	-49.7	-49.0	-47.9	-46.8	-45.2	-42.9	-40.9	-39.6	-38.0					
30	-29.5	-29.1	-30.0	-32.3	-35.6	-37.7	-40.3	-43.3	-44.6	-45.5	-47.5	-49.3	-49.7	-49.4	-48.7	-47.8	-46.2	-44.1	-42.7	-41.7	-40.3					
	-29.9	-29.8	-29.6	-32.0	-35.0	-37.4	-40.1	-43.3	-45.1	-45.6	-46.8	-48.4	-49.6	-49.8	-49.4	-48.6	-47.0	-45.2	-44.2	-43.1	-42.4					
	-29.4	-29.5	-29.8	-31.2	-33.8	-36.7	-41.1	-43.8	-44.6	-45.3	-46.6	-48.3	-49.6	-50.2	-49.8	-49.3	-47.9	-46.4	-45.5	-44.2	-44.1					
	-29.9	-29.4	-29.6	-29.9	-32.0	-34.7	-40.0	-43.4	-43.7	-44.3	-46.4	-49.6	-49.7	-50.2	-50.1	-49.4	-48.5	-47.1	-46.0	-45.4	-45.7					
	-29.8	-29.7	-29.1	-28.6	-30.6	-32.3	-37.0	-41.9	-43.2	-43.9	-45.8	-47.8	-49.4	-50.4	-50.3	-49.7	-49.1	-48.0	-47.0	-46.7	-46.9					
25	-29.7	-29.6	-29.4	-27.8	-29.1	-30.9	-34.8	-38.4	-41.6	-43.6	-45.3	-47.1	-48.5	-49.8	-50.2	-49.7	-49.1	-48.3	-47.8	-47.3	-47.5					
	-29.4	-29.4	-29.6	-26.7	-27.0	-28.6	-32.2	-35.0	-38.7	-42.6	-44.9	-46.3	-48.0	-48.9	-49.5	-49.4	-48.7	-48.1	-48.2	-48.4	-48.4					
	-29.2	-29.5	-29.4	-24.3	-25.2	-26.8	-29.2	-33.2	-37.1	-40.4	-43.9	-46.1	-47.8	-48.1	-48.3	-48.5	-48.3	-48.3	-48.8	-49.0	-49.0					
	-19.0	-20.4	-21.7	-22.5	-23.7	-25.7	-29.7	-34.7	-38.1	-40.4	-44.2	-45.8	-46.4	-47.6	-48.1	-48.1	-48.0	-48.5	-48.7	-48.8	-48.8					
	-20.6	-21.2	-22.5	-23.2	-23.7	-24.6	-27.3	-30.1	-33.5	-40.3	-45.2	-46.5	-46.8	-48.3	-48.6	-49.2	-49.6	-50.5	-50.1	-49.4	-49.0					
20	-18.2	-18.7	-20.3	-22.5	-24.4	-25.4	-26.4	-27.6	-31.0	-35.2	-37.3	-38.9	-41.8	-45.9	-50.5	-55.1	-58.6	-59.6	-57.5	-55.7	-54.4					

Table Five. Geoid Undulations Using Method B with GEM6 Coefficients Truncated at Degree 10 and with a Cap Size of 20°.

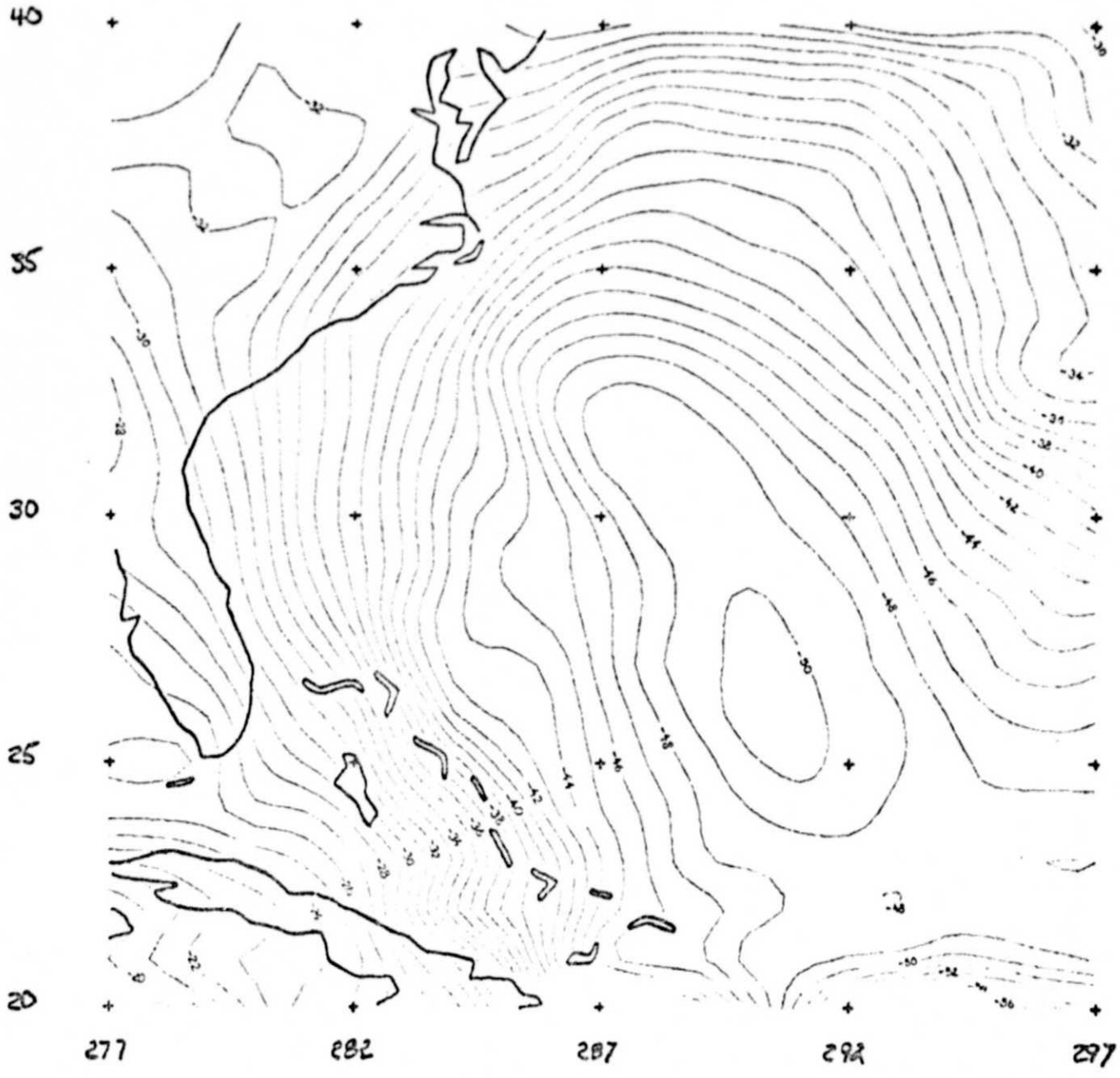

Figure Seven. Geoid Undulation Using Method B with GEM 6 Coefficients Truncated at Degree 16 and with a Cap Size of 20°.

φ \ λ	280							285						290					295		
40	1.1	1.1	1.1	1.1	1.1	1.2	1.2	1.2	1.2	1.2	1.2	1.3	1.3	1.3	1.4	1.5	1.6	1.6	1.6	1.6	1.6
	1.1	1.1	1.1	1.1	1.1	1.2	1.2	1.2	1.2	1.2	1.3	1.3	1.3	1.4	1.5	1.6	1.6	1.6	1.5	1.5	1.6
	1.1	1.1	1.1	1.1	1.2	1.2	1.2	1.2	1.2	1.3	1.3	1.4	1.4	1.5	1.5	1.6	1.5	1.4	1.5	1.5	1.6
	1.1	1.1	1.1	1.1	1.2	1.2	1.2	1.2	1.3	1.4	1.5	1.5	1.5	1.5	1.5	1.6	1.5	1.5	1.5	1.6	1.6
	1.1	1.1	1.1	1.2	1.2	1.2	1.2	1.3	1.4	1.6	1.6	1.6	1.6	1.6	1.5	1.6	1.6	1.6	1.6	1.6	1.6
35	1.1	1.1	1.1	1.2	1.2	1.2	1.2	1.3	1.3	1.4	1.5	1.5	1.6	1.6	1.5	1.5	1.5	1.6	1.6	1.6	1.7
	1.1	1.1	1.2	1.2	1.2	1.2	1.3	1.3	1.4	1.5	1.5	1.5	1.6	1.6	1.6	1.6	1.6	1.6	1.6	1.7	1.8
	1.1	1.2	1.2	1.2	1.2	1.3	1.3	1.5	1.6	1.6	1.6	1.6	1.6	1.6	1.6	1.6	1.6	1.6	1.6	1.7	1.7
	1.2	1.2	1.2	1.2	1.3	1.4	1.6	1.6	1.6	1.6	1.6	1.7	1.7	1.8	1.7	1.7	1.7	1.7	1.6	1.7	1.8
	1.2	1.2	1.2	1.3	1.4	1.6	1.6	1.7	1.6	1.6	1.7	1.7	1.8	1.8	1.8	1.8	1.8	1.8	1.7	1.7	1.8
3	1.2	1.2	1.2	1.3	1.5	1.6	1.6	1.7	1.7	1.7	1.7	1.8	1.9	1.9	1.8	1.8	1.7	1.8	1.8	1.8	1.8
	1.2	1.2	1.2	1.3	1.5	1.6	1.6	1.6	1.7	1.7	1.7	1.7	1.8	1.9	1.8	1.8	1.8	1.8	1.8	1.9	1.9
	1.2	1.2	1.2	1.3	1.4	1.6	1.6	1.6	1.6	1.7	1.7	1.8	1.8	1.8	1.7	1.7	1.7	1.8	1.9	2.0	1.9
	1.2	1.2	1.2	1.3	1.4	1.5	1.6	1.6	1.6	1.7	1.7	1.8	1.8	1.7	1.7	1.7	1.7	1.7	1.9	2.0	1.9
	1.2	1.2	1.3	1.3	1.4	1.5	1.6	1.6	1.6	1.6	1.7	1.7	1.8	1.8	1.8	1.8	1.8	1.8	1.8	2.0	2.1
25	1.3	1.3	1.3	1.3	1.4	1.6	1.6	1.6	1.6	1.6	1.6	1.6	1.7	1.8	1.8	1.8	1.8	1.8	1.8	2.0	2.1
	1.4	1.4	1.3	1.4	1.5	1.5	1.6	1.6	1.6	1.6	1.6	1.6	1.6	1.7	1.7	1.7	1.7	1.6	1.7	1.8	2.0
	1.4	1.4	1.3	1.4	1.5	1.5	1.6	1.6	1.6	1.6	1.6	1.6	1.6	1.6	1.7	1.6	1.6	1.6	1.6	1.7	1.9
	1.3	1.3	1.4	1.4	1.4	1.6	1.6	1.6	1.6	1.6	1.6	1.6	1.6	1.6	1.6	1.6	1.6	1.6	1.6	1.7	1.8
	1.3	1.4	1.4	1.4	1.4	1.5	1.5	1.5	1.6	1.6	1.6	1.6	1.6	1.6	1.6	1.6	1.6	1.6	1.6	1.6	1.7
20	1.3	1.3	1.4	1.4	1.4	1.4	1.4	1.4	1.5	1.5	1.5	1.5	1.5	1.6	1.6	1.6	1.6	1.6	1.6	1.6	1.6

Table Six. Standard Deviations of the Geoid Undulation (Table Five) Using the Potential Coefficient Error Model One.

λ =	280							285						290						295		
φ=40	1.8	1.8	1.8	1.8	1.8	1.8	1.8	1.8	1.8	1.9	1.9	1.9	1.9	2.0	2.0	2.1	2.1	2.2	2.1	2.1	2.2
	1.8	1.8	1.8	1.8	1.8	1.8	1.8	1.8	1.9	1.9	1.9	2.0	2.0	2.0	2.1	2.1	2.1	2.1	2.1	2.1	2.1
	1.8	1.8	1.8	1.8	1.8	1.8	1.8	1.9	1.9	1.9	2.0	2.0	2.0	2.1	2.1	2.1	2.1	2.0	2.1	2.1	2.1
	1.8	1.8	1.8	1.8	1.8	1.8	1.9	1.9	2.0	2.0	2.1	2.1	2.1	2.1	2.1	2.1	2.1	2.1	2.1	2.1	2.2
	1.8	1.8	1.8	1.8	1.8	1.8	1.9	1.9	2.0	2.1	2.1	2.1	2.1	2.1	2.1	2.1	2.1	2.1	2.2	2.2	2.2
35	1.8	1.8	1.8	1.8	1.8	1.9	1.9	1.9	2.0	2.0	2.1	2.1	2.1	2.1	2.1	2.1	2.1	2.1	2.2	2.2	2.2
	1.8	1.8	1.8	1.8	1.9	1.9	1.9	2.0	2.0	2.1	2.1	2.1	2.1	2.1	2.1	2.1	2.1	2.1	2.2	2.2	2.3
	1.8	1.8	1.8	1.9	1.9	1.9	2.0	2.1	2.1	2.1	2.1	2.2	2.2	2.2	2.2	2.2	2.2	2.2	2.2	2.2	2.2
	1.8	1.8	1.8	1.9	2.0	2.0	2.1	2.2	2.2	2.2	2.2	2.2	2.2	2.3	2.2	2.2	2.2	2.2	2.2	2.2	2.3
	1.8	1.8	1.8	1.8	1.9	2.0	2.1	2.2	2.1	2.1	2.2	2.2	2.2	2.2	2.2	2.2	2.2	2.2	2.2	2.2	2.2
30	1.8	1.8	1.8	1.9	2.0	2.1	2.1	2.2	2.2	2.2	2.2	2.2	2.3	2.3	2.2	2.2	2.2	2.2	2.2	2.2	2.2
	1.8	1.8	1.8	1.8	2.0	2.1	2.1	2.1	2.2	2.2	2.2	2.2	2.2	2.3	2.2	2.2	2.2	2.2	2.2	2.3	2.3
	1.8	1.8	1.8	1.8	1.9	2.0	2.1	2.1	2.1	2.2	2.2	2.2	2.2	2.2	2.2	2.2	2.2	2.2	2.3	2.4	2.3
	1.8	1.8	1.8	1.8	1.9	2.0	2.0	2.1	2.1	2.2	2.2	2.2	2.2	2.2	2.2	2.2	2.2	2.2	2.3	2.4	2.3
	1.8	1.8	1.8	1.8	1.9	2.0	2.0	2.1	2.1	2.1	2.2	2.2	2.2	2.2	2.2	2.2	2.2	2.2	2.2	2.4	2.4
25	1.8	1.8	1.8	1.9	1.9	2.0	2.0	2.0	2.1	2.1	2.1	2.1	2.2	2.2	2.2	2.2	2.2	2.2	2.2	2.4	2.4
	1.9	1.9	1.9	1.9	2.0	2.0	2.0	2.1	2.0	2.0	2.1	2.1	2.1	2.2	2.2	2.2	2.2	2.1	2.2	2.2	2.4
	1.9	1.9	1.9	1.9	2.0	2.0	2.1	2.1	2.1	2.1	2.1	2.1	2.1	2.1	2.2	2.1	2.1	2.1	2.1	2.2	2.3
	1.9	1.9	1.9	1.9	1.9	2.0	2.1	2.1	2.0	2.0	2.1	2.1	2.1	2.1	2.1	2.0	2.0	2.0	2.1	2.2	2.2
	1.9	1.9	1.9	1.9	1.9	2.0	2.0	2.0	2.0	2.0	2.0	2.1	2.1	2.1	2.1	2.0	2.0	2.0	2.0	2.1	2.2
20	1.9	1.9	1.9	1.9	1.9	1.9	1.9	1.9	2.0	2.0	2.0	2.0	2.0	2.0	2.0	2.0	2.0	2.0	2.0	2.0	2.1

Table Seven. Standard Deviations of the Geoid Undulation (Table Five) Using the Potential Coefficient Error Model Two.

square root of the variance of the difference being ±1.55 meters. Based on the standard deviations shown in Figure Six, we would expect the above difference to be ±1.3 m when using the optimistic potential coefficient error model and ±1.8 m when using the pessimistic model. (The values are arrived at by computing $\sigma^2_{1\sigma-2\sigma} = \sigma^2_{1\sigma} - \sigma^2_{2\sigma}$). These expected values are very compatible with the result actually found.

In the computation described in the above paragraph, the atmospheric correction was rigorously applied with mean difference between the two results being -0.24 meters. A test computation was made when the atmosphere was not considered in the anomaly data within the 10° and 20° caps. In this case the resulting mean undulation difference was found to be -1.34 meters which is a considerable increase from the -0.24 meters when the atmosphere was properly treated. These results indicate the practical value and need of the atmospheric correction to gravity anomalies when the undulations of the geoid are being computed.

Another computation that was made was with the GEM 6 potential coefficients taken to $\ell = 22$ with a $\psi = 20°$. The resulting undulations were compared to the values computed using the coefficients to $\ell = 16$. The differences between the undulations was a maximum of 0.3 m with a negligible mean difference and variance as is shown in Table Eight.

Table Eight. Comparison of Various Undulation Computations (meters)

	A	B	C	D	E
Mean Diff	.03	-0.24	.03	3.87	4.15
σ	±.09	±1.55	±.18	±2.58	±3.52
Max (+) Diff	0.2	2.9	0.3	12.0	10.4
Max (-) Diff	-0.2	-3.6	-0.3	-0.6	-5.3

A: Difference between Method A minus Method B ($\ell_{max} = 16$, $\psi = 20°$);
B: Difference between Method B($\psi = 20°$) minus Method B ($\psi = 10°$);
C: Difference between Method B($\ell_{max} = 22$) minus Method B($\ell_{max} = 16$);
D: Difference between Method B ($\psi = 20°$)minus solution of Vincent-Marsh;
E: Difference between Method B ($\psi = 10°$)minus solution of Vincent-Marsh.

The final comparison that was carried out was the comparison of the cali-

bration geoid of this report to that geoid of Vincent and Marsh (1973), which was provided to us by Jim Marsh at 1° x 1° corner points. The results of the comparison are shown in Table Eight. Here we see that there is a strong systematic difference in the undulation of 3.87 m, about 1.2 meters of which is caused by the neglect by Vincent and Marsh of the influence of the atmosphere. The square root of the variance of the undulation differences is ±2.58 meters with the largest discrepancy being 12.0 m. (Again part of this latter discrepancy is due to their neglect of the atmosphere). The main cause of the non-systematic differences between the undulations is probably the 1° x 1° gravity data used in the computations.

9. The Zero-Order Undulation

The zero-order undulation of the geoid has been discussed by Heiskanen and Moritz (1967, p. 102) for the case of an undulation computation using Stokes' equation in a global integration process. Specifically we have:

$$N_0 = \frac{k\,\delta M}{2GR} - \frac{R\Delta g_0}{2G} \tag{48}$$

where $k\,\delta M$ is the difference between a true value of the geocentric gravitational constant of the earth plus the atmosphere, and that adopted for the reference field. In addition Δg_0 is the mean gravity anomaly, of those anomalies (after the atmospheric correction has been applied) referred to the adopted constants. Thus:

$$\Delta g_0 = \frac{1}{4\pi} \iint_{\sigma} (\Delta g - \delta g_A)\, d\sigma \tag{49}$$

This Δg_0 must also be subtracted from the Δg° given in (26) to assure that the anomalies used in Stokes' equation have a global average equal to zero. In this case an additional term will appear from (10) and (18) equal to:

$$-\frac{R\Delta g_0}{4\pi G} \iint_{\sigma_0} S(\psi)\, d\sigma = -\frac{R\Delta g_0}{G}\, \mathfrak{F}(\psi_0) \tag{50}$$

Equation (50) is now added to (48) to obtain the modified N_o term that applies for both methods of computation of geoid undulations described in this report. We have:

$$\overline{N}_o = \frac{k\delta M}{2GR} - \frac{R\Delta g_o}{G}\left(\frac{1}{2} + \frac{1}{2}(\psi_o)\right) \tag{51}$$

If ψ_o is 180° we have $N_o = \overline{N}_o$. If $k\delta M$ and Δg_o are zero $\overline{N}_o$ is zero. If $k\delta M = 0$, and $\Delta g_o = 1$ mgal, N_o is -4.6 m for $\psi_o = 10°$ and -5.8 m for $\psi_o = 20°$. The value of Δg_o can be determined from (49) if we have a global gravity field or from:

$$\Delta g_o = \gamma' - \gamma \tag{52}$$

where γ' is the true equatorial gravity based on the mass of the earth plus the atmosphere and γ is the corresponding value adopted for use in the computations.

Thus, we have derived a new N_o term that is cap size dependent. This N_o, if it can be determined, must be added to the undulations obtained from equation (1) or equation (14) to obtain the true undulation with respect to the adopted constants. If N_o is set to zero, the computed undulations will refer to a set of unknown constants such that $k\delta M$ and Δg_o are zero.

10. Summary

This paper documents two procedures that can be used for the computation of geoid undulations combining potential coefficient data and terrestrial gravity data. We found that the two methods yield essentially the same results (at the ±0.09 m level). However, the error analysis for Method B is simpler than that for Method A.

In developing the procedures for each method two important techniques must be used. First, it was found that the atmospheric correction is signifi-

cant and cannot be neglected as its neglect can cause errors in the computed undulation on the order of 2 meters with a truncation cap of 20°. Second, the numerical integration of Stokes' equation must be done in a precise manner or integration errors of about 1 meter will result.

A preliminary error analysis was done considering the error sources due to potential coefficient errors, gravity anomaly errors, and the truncation error caused by taking the potential coefficients to a certain maximum degree only. This analysis indicated that certain cap sizes (around 10°) would give poorer results than more optimum sizes, such as 20°, which was selected for use here.

The actual geoid undulations were computed in the Geos - 3 calibration area using the GEM 6 potential coefficients to degree 16 and the 1° x 1° mean anomalies available in July 1975. The results obtained showed a mean difference of 3.87 m from the Vincent-Marsh geoid with a difference variance of $(2.58\ m)^2$. The estimated standard deviation of the undulations computed here were on the order of 1 to 2 meters with respect to the defined constants. This error analysis neglects the effect of using anomaly blocks of a size smaller than 1° x 1°, and the effect of ellipsoidal correction terms to Stokes' equation.

Although these computations have been done for the GEM 6 coefficients they can easily be repeated for other coefficient sets with a corresponding error analysis provided a realistic variance-covariance matrix for the potential coefficients is available.

References

Cook, A. H., The External Gravity Field of a Rotating Spheroid to the Order e^5, Geophysical Journal, 199-214, 1959.

Gaposchkin, E. M., Earth's Gravity Field to the Eighteenth Degree and Geocentric Coordinates for 104 Stations from Satellite and Terrestrial Data, Journal of Geophysical Res., 79, 5377-5411, 1974.

Groten, E. and Rummel, R., Improved Gravimetric Geoid for $7° \leq \lambda \leq 12°$ (E) and $47° \leq \phi \leq 54°$ (N), Allgemeine Vermessungs-Nachrichten, 7, 263-267, 1974.

Heiskanen, W. and Moritz, H., Physical Geodesy, W. H. Freeman & Co., San Francisco, 1967.

International Association of Geodesy, Publication Spéciale du Bulletin Géodesique, Geodetic Reference System 1967, Paris, 1971.

Lambert, W. D. and Darling, F. W., Tables for Determining the Form of the Geoid and its Indirect Effect on Gravity, U. S. Coast and Geodetic Survey, Special Publication No. 199, Washington, D. C. 1936.

Lerch, F. J., Wagner, C., Richardson, J., Brownd, J., Goddard Earth Models (5 and 6), NASA Document X-921-74-145, Goddard Space Flight Center, Greenbelt, Maryland, 1974.

Marsh, J. and Vincent, S., Detailed Geoid Computations For Geos-C Altimeter Experiment Areas, NASA Document X-592-73-303 Goddard Space Flight Center, Greenbelt, Maryland, 1973.

Molodenskii, M. S., Eremeev, V. F., Yurkina, M. I., Methods for Study of the External Gravitational Field and Figure of the Earth, Israel Program for Scientific Translations, Jerusalem, 1962.

Moritz, H., Die Zukunft der Gravimetrischen Geodäsie, ZfV, No. 1, 15-21., 1975.

Moritz, H., Precise Gravimetric Geodesy, Report No. 219, Department of Geodetic Science, The Ohio State University, Columbus, 1974.

Paul, M. K., A Method of Evaluating the Truncation Error Coefficients for Geoidal Height, Bulletin Geodesique, No. 110, 413-425, 1973.

Rapp, R. H., Accuracy of Geoid Undulation Computations, Journal of Geophysical Research, 78, 7589-7595, 1973.

Rapp, R. H., Comparison of Satellite Geoids and Anomaly Fields, Department of Geodetic Science, Report No. 80, The Ohio State University, Columbus, 1967.

Rapp, R. H., Methods for the Computation of Geoid Undulations From Potential Coefficients, Bulletin Geodesique, 101, 283-297, 1971.

Tscherning, C. C. and Rapp, R. H., Closed Covariance Expressions for Gravity Anomalies, Geoid Undulations, and Deflections of the Vertical Implied by Anomaly Degree Variance Models, Report No. 208, Department of Geodetic Science, The Ohio State University, Columbus, 1974.

Vincent, S. and Marsh, J., Gravimetric Global Geoid, in Proceedings of the International Symposium on the Use of Artificial Satellites for Geodesy and Geodynamics, ed, G. Veis, National Technical University, Athens, Greece, 1974.